



Fixed mesh shape reduces variability in codend size selection

Bak-Jensen, Zita; Herrmann, Bent; Santos, Juan; Jacques, Nadine; Melli, Valentina; Feekings, Jordan P.

Published in:
Canadian Journal of Fisheries and Aquatic Sciences

Link to article, DOI:
[10.1139/cjfas-2022-0049](https://doi.org/10.1139/cjfas-2022-0049)

Publication date:
2022

Document Version
Peer reviewed version

[Link back to DTU Orbit](#)

Citation (APA):
Bak-Jensen, Z., Herrmann, B., Santos, J., Jacques, N., Melli, V., & Feekings, J. P. (2022). Fixed mesh shape reduces variability in codend size selection. *Canadian Journal of Fisheries and Aquatic Sciences*, 79(11), 1820-1829. <https://doi.org/10.1139/cjfas-2022-0049>

General rights

Copyright and moral rights for the publications made accessible in the public portal are retained by the authors and/or other copyright owners and it is a condition of accessing publications that users recognise and abide by the legal requirements associated with these rights.

- Users may download and print one copy of any publication from the public portal for the purpose of private study or research.
- You may not further distribute the material or use it for any profit-making activity or commercial gain
- You may freely distribute the URL identifying the publication in the public portal

If you believe that this document breaches copyright please contact us providing details, and we will remove access to the work immediately and investigate your claim.

1 Fixed mesh shape reduces variability in codend size 2 selection

3 Zita Bak-Jensen^{1*}, Bent Herrmann^{1,2,3}, Juan Santos⁴, Nadine Jacques³, Valentina Melli¹, Jordan
4 P. Feekings¹

5 ¹ DTU Aqua, Technical University of Denmark, Hirtshals, Denmark

6 ² SINTEF Ocean, Brattørkaia 17C, N-7010 Trondheim, Norway

7 ³ The Arctic University of Norway, UiT, Breivika, N-9037 Tromsø, Norway

8 ⁴ Thünen Institute for Baltic Sea Fisheries, Alter Hafen Süd 2, Rostock, 18069; Germany

9 * Corresponding author.

10 E-mail address: zitba@aqua.dtu.dk

11

12 Abstract

13 Diamond-mesh codends are the most commonly used in demersal trawls. However, mesh
14 geometry tends to vary in these codends during fishing, which leads to a less well-defined size
15 selection process. This leaves one questioning the rationality of regulating exploitation patterns
16 based on mesh size when size selection and/or variation between hauls is highly variable. While
17 it has been speculated and theoretically investigated how much the variability in mesh geometry
18 may contribute to the variability in size selection, it remained to be quantified experimentally.
19 Therefore, we conducted field test comparing the size selectivity of a simple diamond-mesh
20 codend, where meshes are subjected to variation in geometry, with a rigid diamond-mesh
21 codend, where the geometry of the meshes were kept constant. For Atlantic cod (*Gadus*
22 *morhua*) the simple diamond-mesh codend was found to have 45% more variation in size
23 selection than the codend with fixed mesh geometry. This confirms theoretical predictions and
24 may guide research towards codend designs with more well-defined size selection properties.

25

26 *Keywords:* Size Selection, Variability, Codend, Diamond-mesh, Mesh geometry

27 **Introduction**

28 Selectivity in towed gears as defined by Wileman et al. (1996) is “*the probability of a fish of a*
29 *given species and size being retained by a gear once it has encountered it*”. The majority of the
30 selection process occurs in the codend, i.e., the end of the trawl where the catch accumulates
31 (Wileman et al. 1996). Diamond-mesh codends are the most widely applied designs and have
32 traditionally been used in the majority of demersal trawl fisheries due to their simple structure
33 and ease of operation (He, 2007; Wienbeck et al. 2011; Sistiaga et al. 2021). However, multiple
34 studies have shown that diamond-mesh codends do not maintain a constant mesh openness
35 while trawling, due to their flexibility (e.g., Robertson and Stewart, 1988; Reeves et al. 1992;
36 Herrmann, 2005). As the catch accumulates the openness of the meshes along the length of the
37 codend becomes more heterogeneous, whereby meshes close to the catch build-up zone become
38 more open and meshes further forward in the codend become more elongated (i.e., closed) (e.g.,
39 Jones, 1963; Herrmann, 2005; Herrmann and O’Neill, 2005). Since codend size selectivity is
40 largely determined by the openness of the meshes (Jones, 1963; Herrmann et al. 2009), the
41 variations in the openness occurring during the catching process have been associated to the
42 variation of the size selection properties of the codend either at haul level (Herrmann, 2005) or
43 between-hauls (Fryer, 1991; Herrmann and O’Neill, 2005). This applies especially to roundfish,
44 which have a better chance of escaping when the opening angle (OA) is closer to 90° (e.g.,
45 Atlantic cod (*Gadus morhua*); Herrmann et al. 2009).

46
47 Codend size selection is often described by a sigmoid selection curve as a function of length of
48 the fish (Wileman et al. 1996). The desired selection curve would have a knife-edged shape
49 with the critical length at the point above which all fish are retained, and below which all fish
50 are released. However, this is rarely the case as there are several factors (e.g., towing speed,
51 and weight of the catch) that determine whether individuals escape (Roda et al. 2019). A
52 measure for the sharpness of the size selection is the selection range (SR). The selection range
53 is the difference in length between fish with a 75% probability of retention (L75) and the length
54 of fish with a 25% probability of retention (L25) (Wileman et al. 1996). Herrmann (2005) and
55 Herrmann and O’Neill (2005) theorized that variations in the geometry of diamond meshes that
56 result from catch accumulation, impacts the SR obtained. Therefore, if the hypothesis arising
57 from these theoretical studies is true, the more variation in mesh geometry, the larger the SR.
58 Conversely, with more constant mesh openness during fishing, the sharper the resulting
59 selection curve will be.

60 From a management point of view a knife-edged shape selection curve that corresponds to the
61 minimum landing size is desired since it ensures unwanted catches are limited and economic
62 yields are maximized (Andersen, 2019). However, this is rarely the case for fisheries whose
63 exploitation patterns are defined by the size selectivity of diamond-mesh codends, probably due
64 to the variability in mesh geometry impacting on the SR of the codend. Therefore, the geometric
65 variability of codend meshes challenges the management of the exploited fish stocks, as the
66 selection becomes less sharp (i.e., the retention of undersized, and the loss of legal sized
67 individuals is greater). As a result of the suboptimal size selection by the codend alone, some
68 fisheries have supplemented this with additional selective devices to achieve a sharper selection
69 curve such as the grid systems 'Flexigrid' commonly used in the Barents Sea demersal trawl
70 fishery or square mesh panels like BACOMA used in Baltic Sea (Sistiaga et al. 2010 and
71 Wienbeck et al. 2014). However, a better approach could be to stabilize the selection process
72 in the codend, thus avoiding the need for additional selection devices as they often require more
73 handling and increase the cost (Sistiaga et al. 2021).

74
75 The benefit of stabilizing mesh OA has been speculated on theoretically in the past (e.g.,
76 Herrmann, 2005), but has never been tested experimentally. In this study we aimed at
77 quantifying experimentally the effect of OA variability on the sharpness of codend size
78 selection. Therefore, we developed and tested a rigid codend structure, that allowed the mesh
79 OA to be kept constant. This experimental codend was tested in the Baltic Sea and size-
80 selectivity data were collected for cod (*Gadus morhua*). For the first time, to our knowledge,
81 the assumption was tested for proof of concept at sea.

82 83 **Materials and methods**

84 *2.1 Fishing gears*

85 The covered codend method according to Wilemann et al. (1996) was applied. A TV300/60
86 bottom trawl was used, in conjunction with two Thyboron Type 2 (1.78 m²) trawl doors and
87 100 m sweeps. A rigid steel frame was constructed with the dimensions 2 x 0.75 x 0.75 m
88 (length, width and height, respectively; 1.125 m³). The length of the frame was kept short to
89 make handling easier. The frame was made using square profile pipes of 40 mm x 40 mm x 4
90 mm steel (height x width x thickness). The four rectangular surfaces were covered with a 5 mm
91 euroline single twine diamond mesh netting of fixed opening angles. The desired 40° opening
92 angle was achieved by attaching the netting with a specific hanging ratio and controlled with

93 an angle measure. The angle of 40° was chosen as it is in the middle of the normal range of the
94 opening angles in a standard flexible codend (Herrmann et al. 2009). Twenty meshes were
95 randomly chosen for each panel from photographs and the OA was estimated after the fishing
96 trials using the software FISHSELECT (Herrmann et al. 2009). Specifically, individual meshes
97 were digitized and a diamond shape model was fitted to obtain values for OA by use of image
98 analysis facilities in the FISHSELECT software. The closing end of the codend and the 4-meter
99 extension piece (measured as stretch length) ahead of the frame were constructed out of
100 diamond meshes with a nominal mesh size of 50 mm to ensure that the selection process would
101 only occur through the larger meshes mounted on the sides of the rigid codend. Therefore, the
102 total length of the extension piece and the rigid codend was 6 m. The frame was lifted by six
103 floats attached to the longitudinal upper bars of the frame to make sure it was free from the
104 seabed and the codend cover (Figure 1). This codend will from this point forward be denoted
105 as “fixed mesh codend”.

106



107

108 Figure 1. Picture of the rigid frame with the fixed meshes (Fixed mesh codend).

109

110 The standard diamond mesh codend (hereafter referred to as the “flexible mesh codend”) was
111 made of two panels with a circumference of 86 open meshes. The mesh sizes in the codends
112 were measured using an OMEGA-gauge with 125 N stretching force for 20 meshes (dry
113 conditions). The mesh size of the fixed mesh codend, measured in the aft end where there were
114 some loose meshes, was $111.5 \text{ mm} \pm 2.14 \text{ mm}$ (mean \pm standard deviation). The mesh size of
115 the flexible mesh codend was $112.4 \text{ mm} \pm 2.72 \text{ mm}$ (mean \pm standard deviation). The cover

116 (cc) was made of single 2.5 mm-PE twine with a nominal mesh size of 55 mm. It had a stretched
117 length of ~16 m (2.6 x the length of the extension piece and rigid codend combined) and a
118 diameter of ~3 m. To prevent the cover from masking the selectivity of the codend, a total of
119 seven kites were attached to the cover. Five kites were attached to the forward section and the
120 remaining two were attached to each side of the cover.

121

122 *2.2 Experimental fishing and data collection*

123 The experimental fishing trials were conducted in the Baltic Sea onboard the German *FRV*
124 *Solea* (42.40 m LOA, 1780 kW), during the 16th to the 27th of September 2021. The
125 experimental hauls conducted were spatially distributed across German and Danish fishing
126 grounds between ICES Subdivisions 22 and 25. The experimental codends were tested one at a
127 time for a number of hauls. Individuals escaping from the experimental codends (cd) were
128 collected using a cover surrounding the entire codend (Wienbeck et al. 2011, 2014). The catches
129 obtained at haul level were treated for each compartment separately. The fish retained in the
130 codend and the escapees in the cover were kept separate and sampled one after another. The
131 total length of all cod individuals were measured and rounded down to the centimeter below
132 using measuring boards.

133

134 *2.3 Estimation of codend selectivity*

135 The size selection data obtained by each of the experimental codends was analyzed using the
136 methodology described in Wileman et al. (1996). With this methodology, it is assumed that (a)
137 the proportion of the fish retained in the codend is determined by the ability of the fish to pass
138 through the codend meshes, and (b), that such ability is determined mostly by the morphology
139 and size of the fish, and the geometry and size of the meshes. These basic assumptions allow
140 modeling the codend retention probability $r(l)$ by simple mathematical functions with
141 parametric structures leading to non-decreasing, s-shaped selectivity curve asymptotically
142 restricted to values between [0.0, 1.0] (Wileman et al. 1996). The *logistic*, *probit*, *gompertz*,
143 and *Richards* selectivity models were considered as candidates:

Can. J. Fish. Aquat. Sci. Downloaded from cdnsciencepub.com by Danmarks Tekniske Informationscenter on 06/17/22
For personal use only. This Just-IN manuscript is the accepted manuscript prior to copy editing and page composition. It may differ from the final official version of record.

$$r(l, \mathbf{v}) = \left\{ \begin{array}{l} \text{logistic}(l, L50, SR) = \frac{\exp\left(\frac{\ln(9)}{SR} \times (l - L50)\right)}{1.0 + \exp\left(\frac{\ln(9)}{SR} \times (l - L50)\right)} \\ \text{Probit}(l, L50, SR) \approx \Phi\left(\frac{1.349}{SR} \times (l - L50)\right) \\ \text{Gompertz}(l, L50, SR) \approx \exp\left(-\exp\left(-\left(0.3665 + \frac{1.573}{SR} \times (l - L50)\right)\right)\right) \\ \text{Richards}(l, L50, SR, \delta) = \left(\frac{\exp\left(\text{Logit}(0.5^\delta) + \left(\frac{\text{Logit}(0.75^\delta) - \text{Logit}(0.25^\delta)}{SR}\right)(l - L50)\right)}{1.0 + \exp\left(\text{Logit}(0.5^\delta) + \left(\frac{\text{Logit}(0.75^\delta) - \text{Logit}(0.25^\delta)}{SR}\right)(l - L50)\right)}\right)^{1/\delta} \end{array} \right.$$

144 =

where
 $\text{Logit}(r) = \ln\left(\frac{r}{1.0 - r}\right)$

145 (1)

146 The term Φ in the probit function refers to the cumulative distribution function of a standard
 147 normal distribution. $\mathbf{v} = (L50, SR)$ are the parameters that control the shape of the selection
 148 curve. Note that the *Richards* model involves an additional parameter δ which adds flexibility
 149 to the selection curve. The expected number of fish retained in the codend (n_{cd_l}) and the number
 150 of escapees collected in the cover codend (n_{cc_l}) can be directly related to the total number of
 151 fish entering the codend n_l and the selection curve:

$$\begin{aligned} n_{cd_l} &= n_l \times r(l, \mathbf{v}) \\ n_{cc_l} &= n_l \times (1.0 - r(l, \mathbf{v})) \end{aligned} \quad (2)$$

152
 153
 154 Under the assumption that the retained and escaped fractions are determined by the size
 155 selection of the codend, the selection curves described in Eq. 1 and associated selectivity
 156 parameters can be estimated via Maximum Likelihood, by minimizing the negative of the log-
 157 likelihood function derived from the binomial probability mass function:
 158

$$\text{LogLik} = -\sum_{i=1}^m \sum_l \{n_{cd_{il}} \times \ln(r(l, \mathbf{v})) + n_{cc_{il}} \times \ln(1.0 - r(l, \mathbf{v}))\} \quad (3)$$

160
 161

162 The log-likelihood function (Eq. 3) include a summation over hauls $h \in \{i=1, \dots, m\}$, with $n_{cd_{il}}$
 163 and $n_{cc_{il}}$ being the number of cod sampled in haul i belonging to length class l . Thus, assuming
 164 that the m hauls were randomly drawn from all possible hauls that could be conducted, Eq. 3
 165 returns an estimate of the population-average selectivity properties of the codend tested.

166 The four models described in Eq. 1 were estimated and ranked by AIC (Akaike, 1974), and the
 167 model with lowest AIC was picked for further analysis.

168
 169 To account for potential variability within and between hauls of the size-selection process, we
 170 used the double bootstrap method (Efron, 1979; Millar, 1993; Sistiaga et al. 2010) as follows:

171 a) Based on the observed hauls, $H = h_{i=1}, \dots, h_m$, a random sample of hauls $H^* = h_{i=1^*}, \dots, h_{m^*}$
 172 is generated by non-parametric resampling. In other words, after selecting haul i , this is
 173 replaced in the original sample so that it can be resampled. This outer resampling
 174 scheme emulates the between-haul variation in the size selectivity data.

175 b) A second, inner resampling scheme is applied to the length distribution of the measured
 176 fish, separately for each haul drawn in Step (a) and within the haul. For cover-codend
 177 data, this step generates bootstrap distributions of lengths of measured fish in the codend
 178 ($n_{cd^*_{il}}$) and cover ($n_{cc^*_{il}}$) by resampling the data in each length class independently.
 179 Once this step is concluded, a new sample $H^{**} = h_{i=1^{**}}, \dots, h_{m^{**}}$ is generated from the
 180 original data.

181 c) Selectivity estimates from the bootstrap data generated in the two previous steps are
 182 obtained using Maximum Likelihood (Eq. 3), resulting in a selectivity curve $r^*(l, \nu^*)$
 183 and associated parameters $\nu^* = (L50^*, SR^*, (\delta^*))$.

184 d) Steps (a)–(c) B are repeated $B=10.000$ times, so that a bootstrap population of selectivity
 185 curves $r^{*b}(l)$, and associated selectivity parameters ($L50^{*b}, SR^{*b}(\delta^{*b})$) are generated
 186 ($b=1, \dots, B$).

187 The distributions of the average selectivity curve and associated parameters estimated in
 188 Equation 3 are approximated by the histogram based on the population of size B generated in
 189 Step (d), from which 95% confidence intervals are obtained using the percentile method (Efron,
 190 1979).

191 192 2.4 Evaluation of differences in selectivity among tested codends

193 Assuming that the variation in the geometry of the codend meshes is a major contributor for the
 194 variability of the size selection of the codend and that such variability is reflected on the value
 195 of the SR (Herrmann, 2005, Herrmann and O'Neill 2005), then the average SR value estimated

196 by pooling the m hauls conducted with a given codend should contain the variation of the size
 197 selection caused by mesh geometry variations occurring at haul level and across hauls (Fryer
 198 1991; Herrmann and O'Neill 2005). Thus, the larger the SR the larger the combined within-
 199 and-between haul variability and the reduced steepness of the selection curve. By testing the
 200 selective properties of a simple diamond mesh codend with flexible meshes and an experimental
 201 codend with the geometry of the meshes fixed, the contribution of geometric mesh variation to
 202 selectivity variability is quantified by the following statistics:

$$203$$

$$204 \Delta SR[cm] = (SR_{D2} - SR_{D1})$$

$$205 \Delta SR[\%] = 100 \times \frac{(SR_{D2} - SR_{D1})}{SR_{D1}} \quad (5)$$

206 Where SR_{D2} is the selection range estimated for the flexible mesh codend and SR_{D1} is the
 207 selection range estimated for the fixed mesh codend and used as baseline. Therefore, ΔSR
 208 quantifies the contribution of the mesh geometric variability in absolute (cm) and percentage
 209 (%) terms. A value of $\Delta SR \sim 0$ would imply that the variation in selectivity obtained
 210 experimentally could not related to the flexible nature of the codend meshes. Conversely, the
 211 larger the value of ΔSR the larger the contribution of geometric mesh variation to the overall
 212 selectivity variation. To assess if the value of ΔSR is significantly different from zero (either in
 213 absolute or percentage terms), the 95% confidence intervals are estimated from a bootstrap
 214 distribution of ΔSR derived from the previously estimated bootstrap distributions for SR_{D1} and
 215 SR_{D2} (Larsen et al. 2018; Herrmann et al. 2018). Thus, significant differences would be found
 216 when the 95% confidence intervals around ΔSR do not overlap the value associated to the null
 217 hypothesis $H_0: \Delta SR = 0.0$. This procedure is equivalent to methodologies often applied to assess
 218 differences between selectivity and catch comparison curves (Herrmann et al. 2018; Larsen et
 219 al. 2018; Melli et al. 2020).

220

221 **Results**

222 *3.1. Description of fishing operations and catches*

223 A total of 55 hauls were conducted of which 32 hauls were made with the fixed mesh codend
 224 and 23 hauls with the flexible mesh codend. Of these, 27 hauls (12 and 15 for the fixed mesh
 225 codend and flexible mesh codend, respectively) were considered valid and used in the statistical
 226 analysis, as they contained more than 20 cod in total (Table 1). The depth varied between 19
 227 and 46 m and the haul duration varied between 20 and 60 min (Table 1).

228

229 Table 1. Overview of the operational data from each haul used in the analysis. *Denotes missing values

Trawl configuration	Date and time (yyyy/mm/dd hh:mm UTC)	Towing time (min)	Depth (m)	Towing speed (kt)	Number of cod		Total catch cd (kg)
					ncd	ncc	
Fixed mesh	2021/09/19 06:43	20	18	4	12	12	24.09
codend	2021/09/19 12:08	35	18	4	20	9	15.18
	2021/09/20 05:35	35	18	4	19	11	34.84
	2021/09/20 07:04	60	21	3	5	56	124.46
	2021/09/20 10:09	45	18	4	12	8	48.00
	2021/09/20 11:21	50	18	4	13	12	78.50
	2021/09/20 12:36	50	19	4	102	22	104.81
	2021/09/28 05:35	40	18	4	12	41	161.95
	2021/09/28 07:14	60	17	4	1	19	48.73
	2021/09/28 10:10	50	18	4	8	21	133.44
	2021/09/29 04:56	50	19	4	8	177	78.06
	2021/09/29 06:10	50	18	4	7	43	*
Flexible mesh	2021/09/21 05:35	50	20	4	4	25	210.05
codend	2021/09/21 07:08	50	22	4	5	16	170.87
	2021/09/21 10:10	50	19	4	4	57	117.8
	2021/09/21 11:36	50	18	4	20	29	98.96
	2021/09/22 12:02	30	19	4	0	26	108.23
	2021/09/25 13:16	20	33	4	0	20	108.13
	2021/09/25 14:11	20	40	4	10	36	254.18
	2021/09/26 05:33	20	18	4	9	31	69.61
	2021/09/26 06:23	40	20	5	0	43	123.26
	2021/09/26 10:10	50	22	4	4	40	318.93
	2021/09/26 12:06	50	20	4	4	32	190.04
	2021/09/27 05:34	50	26	4	8	18	199.65
	2021/09/27 07:19	50	19	3	4	22	311.07
	2021/09/27 10:10	50	23	4	2	73	153.81
	2021/09/27 11:23	50	18	4	7	17	163.97

230

231 The number of cod used in the analysis and the length range represented in the data for the fixed
 232 mesh codend and flexible mesh codend, respectively, is shown in Table 2.

233

234 Table 2. Overview of the number of cod caught in the codend and the cover and in total used in the analysis for
 235 the fixed mesh codend and flexible mesh codend respectively.

	Number of cod			Length Range (cm)	
	cd	cc	Total	cd	cc
Fixed mesh codend	219	431	650	9 - 48	9 - 33
Flexible mesh codend	81	485	566	9 - 57	8 - 44

236
 237 The OA for the fixed mesh codend was estimated to 39.1° with a standard deviation of 2.4°.
 238 The OA varied from 32.7° to 45.5°.

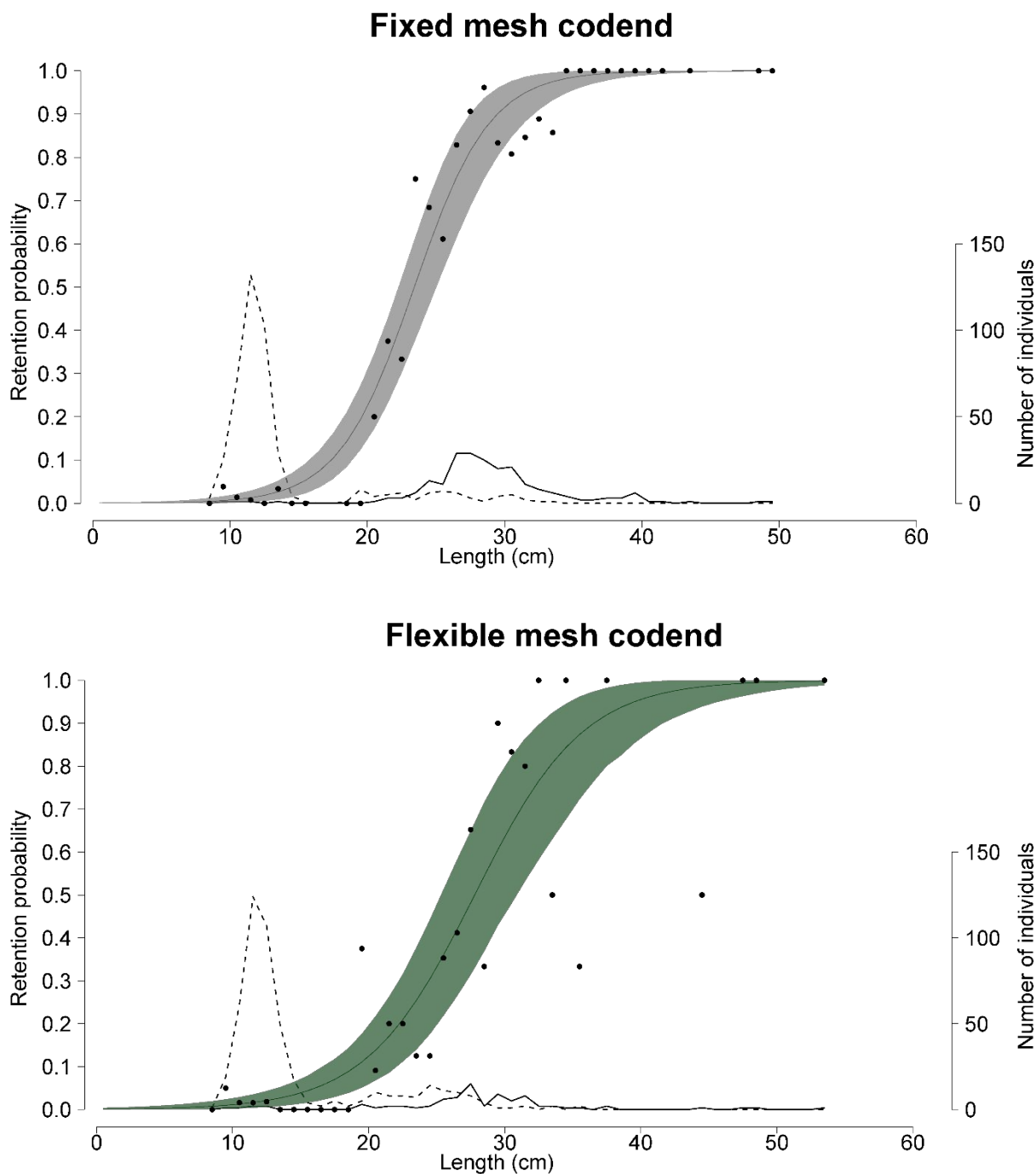
239
 240 *3.2 Covered codend analysis*

241 The logistic model described in Eq. 1 was fitted to the data for both codends (Figure 2) as this
 242 resulted in the lowest AIC value in both cases (Table 3). The fit statistics are reported in Table
 243 4. The SR was found to be 8.75 cm and 6.04 cm for the flexible mesh codend and the fixed
 244 mesh codend respectively (Figure 3). The cumulative probability is shown in Figure 4 for the
 245 SR in percentage. Eq. 5 was used to calculate the difference in SR at 2.7 cm or 44.8 % (Table
 246 5). Thereby, 44.8 % more variation in the size selection was found in the flexible mesh codend
 247 compared to the fixed mesh codend. The L50 was larger for the flexible mesh codend than the
 248 fixed mesh codend (27.79cm and 23.42cm, respectively).

249
 250 Table 3. Overview of the AIC values for flexible mesh and fixed mesh codend respectively. The lowest AIC value
 251 is marked in bold

	AIC value	
	Fixed mesh codend	Flexible mesh codend
Logistic	290.50	273.14
Probit	293.25	274.95
Gompertz	296.45	275.87
Richards	290.71	274.11

252
 253



254

255

256 Figure 2. Length-dependent probabilities of escape in the fixed mesh and flexible mesh codend respectively. The

257 solid curves represent the models fitted to the data (points) with the 95% CIs (shaded area). The frequency curves

258 represent the number of fish caught in each length class in the codend (solid) and cover (dashed).

259

260 Table 4. Fit statistics obtained from the covered codend analysis showing the L50 and SR for the two different

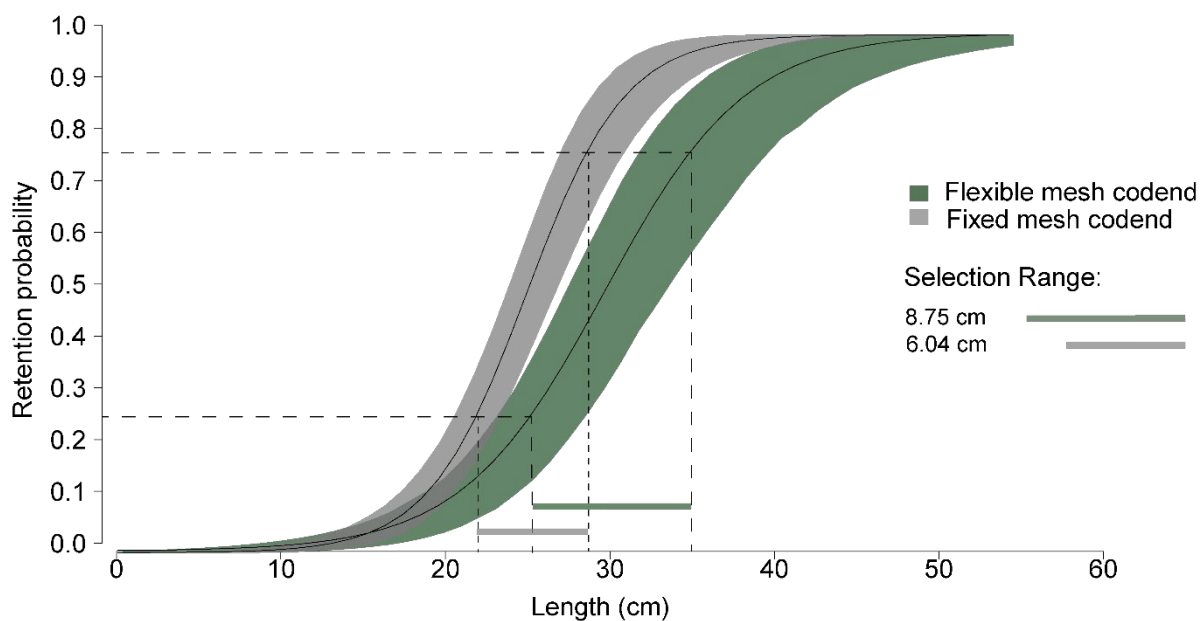
261 trawl configurations tested. Values in parentheses represent 95% CI's. The fit statistics in terms of the p-value,

262 deviance, and DOF.

Flexible mesh codend	Fixed mesh codend
----------------------	-------------------

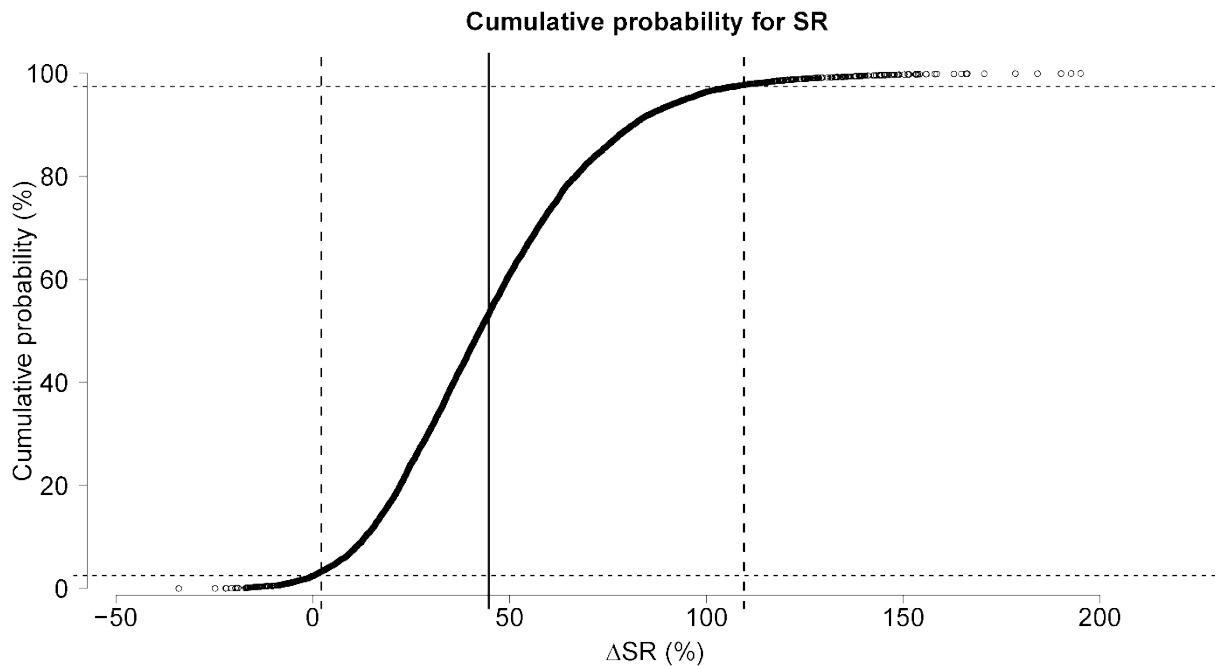
263	L50 (cm)	27.79 (25.21-30.70)	23.42(22.30-25.07)
264	SR (cm)	8.75 (6.80-11.62)	6.04(4.74-7.48)
265	P-value	0.17	0.58
266	Deviance	38.56	30.82
267	DOF	31	33

Selection for Fixed mesh codend and Flexible mesh codend



271
272 Figure 3. Comparison of the estimated length-dependent probabilities of retention for the two codend
273 configurations tested. Dashed lines denote the selection range with results shown in the right side of the figure.
274 Shaded areas represent the 95% CIs.

275



276
277 Figure 4. Comparison of the SR for the two tested configurations in percentage. Vertical stippled lines represent
278 the 95% CIs and the solid line the mean, and the dashed horizontal lines denote the quantile (0.025 and 0.975).
279

280 Table 5. Difference in the selection range between the two different codend configurations. Values in parentheses
281 represent 95% CIs.

282	ΔSR (cm)	2.7 (0.2-5.9)
283	ΔSR (%)	44.8 (2.2-109.6)

285

286 Discussion

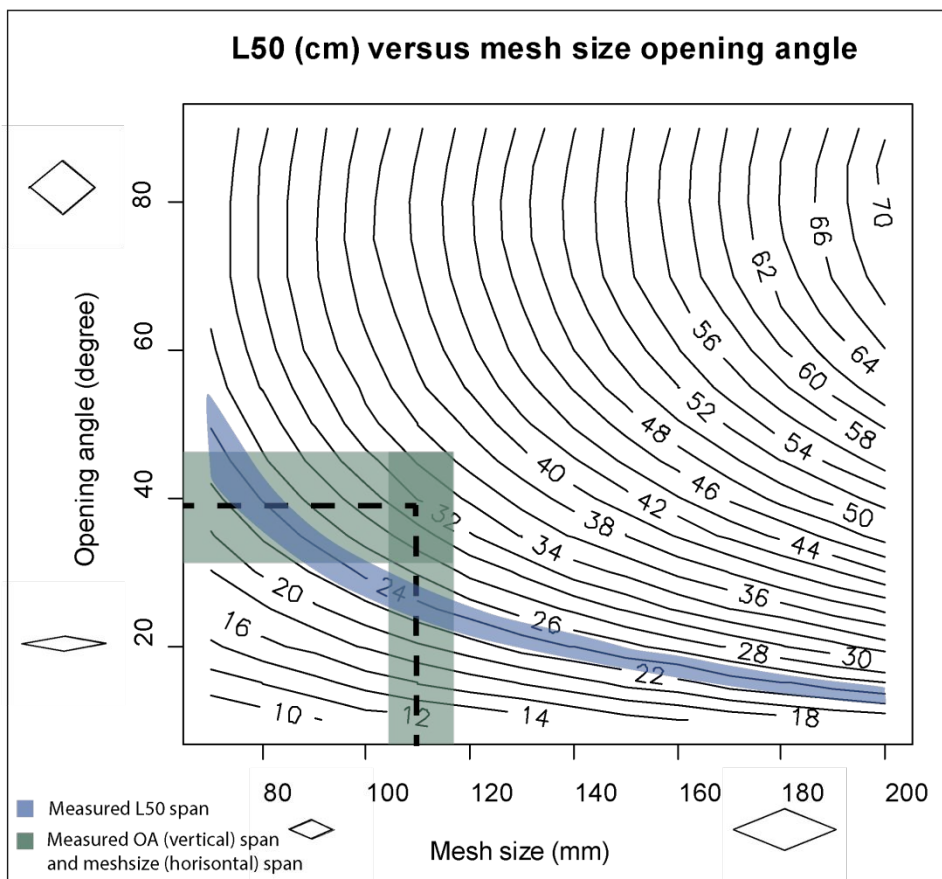
287 We developed and tested a construction that ensured mesh openness remained constant, making
288 it possible to quantify how much variation in mesh geometry influences the ability for fish to
289 escape. This was, to our knowledge, the first time this has been experimentally tested. Our
290 results show that the flexible mesh codend had a much higher variation when compared to the
291 fixed mesh codend. It is important to notice that, while the rigid frame allowed us to
292 successfully demonstrate the effect of mesh openness variation on SR for diamond mesh
293 codend, it is not a commercially or practically viable design.

294 Due to the manufacturing process, i.e., variation in mesh size, it was not possible to keep the
295 OA completely uniform, as it varied between individual meshes from 32.7° to 45.5°. With the
296 OA still subjected to variation, it might be possible to further reduce the SR if the OA can be
297 kept completely constant. Furthermore, catch weights were in general small and did not vary
298 considerably. Bigger and more variable catches could be expected to lead to a higher SR for

299 both codends. However, due to that higher catch weights will result in more variation in mesh
 300 openness for a flexible mesh codend (Herrmann et al. 2005; Herrmann and O'Neill, 2005), it is
 301 expected that SR for this codend is more affected by catch weight than the fixed mesh codend
 302 consequently resulting in a bigger difference in SR between the two codends with increase in
 303 catch weights. Therefore, our estimate of the differences in SR between the two codends is
 304 likely at the lower limit. With larger catches, the setup might reach operational challenges as
 305 the length of the selective part of the fixed mesh codend would be too short.

306

307 The L50 was higher for the flexible mesh codend compared to the fixed mesh codend. However,
 308 that was expected as an OA of approximately 40° prevents meshes from reaching maximum
 309 stretched openness and thereby the chance for escape for larger fish is less in the fixed mesh
 310 codend. With the theoretical estimates of the OA (avg: 39.1° , min: 32.7° and max: 45.5°) and
 311 the measured mesh size (avg: 111.5mm, max: 116mm and min: 105mm), the L50 was found to
 312 vary from 26 cm to 35 cm according to the design guide presented by Herrmann et al. (2009) (
 313 Figure 5).



314

315 Figure 5. Comparison of the estimated L50 for cod and the design guide represented in Herrmann et al. (2009).

316 The horizontal rectangle represents the interval between the maximum and minimum measured OA from the fixed

317 mesh codend. The vertical square represents the span between the maximum and minimum mesh size measured
318 on the fixed frame. The overlapping area of the squares represents where the L50 theoretically would be covered.
319 Dashed lines denote the average OA and mesh size. The colored area along the meso lines denotes the span of the
320 measured L50.

321
322 The difference between the measured L50 interval between the fixed mesh codend and the
323 calculated mesh opening angle and size was found to align unsatisfactory with the design guide
324 presented by Herrmann et al. (2009) (Figure 5). This could be explained by the way the fish
325 approach and contact the mesh. Mesh penetration has both a mechanical and behavioral
326 component (Glass et al. 1993). Krag et al. (2014) found the contact angle of the individual to
327 the mesh opening and the orientation of it to affect the size selection of Antarctic krill
328 (*Euphausia superba*). The design guide in Figure 5 is based on the fish being orientated
329 optimally for escape and penetrating the mesh perpendicular. However, if the fish contact the
330 mesh at another angle, the mesh will appear smaller and the fish might not be able to escape
331 (Krag et al. 2014; Cuende et al. 2020). Furthermore, the end of the fixed mesh codend is made
332 from a small mesh size that is not permeable for escape, and consequently the likelihood of the
333 fish contacting the mesh opening perpendicularly is, therefore, likely to be less. Cuende et al.
334 (2020) found for blue whiting (*Micromesistius poutassou*) that a non-optimal contact angle and
335 orientation affects the L50 and SR making it lower and higher, respectively. This could indicate
336 that the influence of the constant mesh openness is even higher.

337
338 Rather than developing new and more complex gear designs to achieve a sharper selection, our
339 results show that it is possible by simply stabilizing mesh geometry. By testing the influence of
340 variability in OA, we have opened for development towards more rigid codend designs. In
341 contrast to these findings, Vincent et al. (2021) found that deformable meshes may offer greater
342 escape potential than rigid ones. However, despite the escape potential for rigid meshes being
343 less, they offer a more accurate size selection for round fish. Gear specifications that have been
344 found to influence selectivity and subsequently implemented in regulations, such as twine
345 thickness and number of twines, become obsolete with the use of rigid meshes, something that
346 can potentially simplify management regulations. Furthermore, our results open for innovation
347 of new materials and designs, as well as investigation of established approaches such as the
348 flexible grid designs (Lomeli and Wakefield, 2013; Lomeli et al. 2017) that can help maintain
349 a constant escape openness and achieve a sharper size selection.

350

351 With more constant mesh openings, fish morphology becomes even more relevant in the
352 selection process. This will be particularly important when dealing with mixed species fisheries,
353 where the mesh shape should account for the retention or escape of multiple shapes and sizes.
354 For the demersal fisheries in the Baltic Sea, the flatfish species are especially important, as the
355 cod stock is at a critically low level (Santos et al. 2022). Therefore, larger mesh opening angles
356 need to be explored as flatfish theoretically would be more likely to be retained by larger mesh
357 openings than roundfish (Herrmann et al. 2013). Furthermore, T90 mesh codends should be
358 investigated for obtaining less variable selection as these codends have previously been
359 indicated to have lower SR values compared to a simple diamond mesh codend due to their
360 assumed higher stability in mesh openness (Wienbeck et al. 2011).

361

362 **Acknowledgments**

363 The authors would like to thank the crew onboard the “*R/V Solea*”, as well as Kerstin Schöps
364 and Beate Büttner, for their valuable help during the sea trial period. This work has received
365 funding from the European Maritime and Fisheries Fund (EMFF) and the Ministry of Food,
366 Agriculture and Fisheries of Denmark (Ministeriet for Fødevarer, Landbrug og Fiskeri) as part
367 of the projects (FastTrack II – Sustainable, cost effective and responsive gear solutions under
368 the landing obligation (33112-P-18-051) and Udvikling af SELEKTive redskaber og
369 teknologier til kommercielle fiskerier (SELEKT)). Further, we thank the editor and the three
370 anonymous reviewers for the useful comments, which has helped to improve the final
371 manuscript.

372

373 **Competing interests**

374 The authors declare there are no competing interests.

375

376 **Data availability**

377 Raw data were generated at DTU Aqua. Derived data supporting the findings of this study are
378 available from the corresponding author zitba@aqua.dtu.dk on request.

379 **References**

380 Akaike, H., 1974. A new look at the statistical model identification. IEEE Trans.
381 Automat.Contr. 19 (6), 716–723.

- 382 Andersen, K. H. 2019. Fish Ecology; Evolution and Exploitation: A New Theoretical Synthesis.
383 Oxfordshire: Princeton University Press
- 384 Cuende, E., Arregi, L., Herrmann, B., Sistiaga, M., Aboitiz, X., 2020. Prediction of square mesh
385 panel and codend size selectivity of blue whiting based on fish morphology. ICES Journal
386 of Marine Science (2020), 77(7-8), 2857–2869. doi:10.1093/icesjms/fsaa156
- 387 Efron, B. 1979. Bootstrap methods: another look at the jackknife. The Annals of Statistics, 7:
388 1–26.
- 389 Fryer, R.J. 1991. A model of between-haul variation in selectivity. ICES J. Mar. Sci. 48: 281–
390 290. doi:10.1093/icesjms/48.3.281.
- 391 Glass, C.W., Wardle, C.S. and Gosden, S.J., 1993. Behavioural studies of the principles
392 underlying mesh penetration by fish. In ICES Marine Science Symposia (Vol. 196, pp.
393 92-97).
- 394 He, P., 2007. Selectivity of large mesh trawl codends in the Gulf of Maine: I. Comparison of
395 square and diamond mesh. Fisheries Research, (2007), 44-59, 83(1). doi:
396 10.1016/J.FISHRES.2006.08.019
- 397 Herrmann, B., 2005. Effect of catch size and shape on the selectivity of diamond mesh cod-
398 ends. II. Theoretical study of haddock selection Fish. Res., 71 (2005), pp. 15-26
- 399 Herrmann, B. and O'Neill, F.G. 2005. Theoretical study of the between-haul variation of
400 haddock selectivity in a diamond mesh cod-end. Fish. Res. 74: 243-252.
401 doi:10.1016/j.fishres.2005.01.022.
- 402 Herrmann, B., Krag, L.A., Frandsen, R.P., Madsen, N., Lundgren, B., and Stæhr, K.J. 2009.
403 Prediction of selectivity from morphological conditions: methodology and a case study
404 on cod (*Gadus morhua*). Fish. Res. 97: 59-71. doi:10.1016/j.fishres.2009.01.002.
- 405 Herrmann, B., Krag, L. A., & Krafft, B. A. (2018). Size selection of Antarctic krill (*Euphausia*
406 *superba*) in a commercial codend and trawl body. Fisheries Research, 207, 49– 54.
407 <https://doi-org/10.1016/j.fishres.2018.05.028>
- 408 Herrmann, B, Sistiaga, M., Larsen, R. B., Nielsen, K. N., Grimaldo, E., 2013. Understanding
409 sorting grid and codend size selectivity of Greenland halibut (*Reinhardtius*
410 *hippoglossoides*) Fisheries Research 146 (2013) 59– 73
- 411 Jones, R. 1963. Some theoretical observations on the escape of haddock from a codend. ICNAF
412 Spec. Publ. No. 5, 116-127
- 413 Krag, L. A., Herrmann, B., Iversen, S. A., Enga's, A., Nordrum, S., and Krafft, B. A. 2014.
414 Size selection of Antarctic krill (*Euphausia superba*) in trawls. PLoS One, 9: e102168.

- 415 Larsen, R. B., Herrmann, B., Sistiaga, M., Brinkhof, J., & Grimaldo, E. (2018). Bycatch
416 reduction in the Norwegian Deep-water Shrimp (*Pandalus borealis*) fishery with a double
417 grid selection system. *Fisheries Research*, 208, 267– 273. [https://doi-org.
418 /10.1016/j.fishres.2018.08.007](https://doi-org./10.1016/j.fishres.2018.08.007)
- 419 Lomeli, M. J. M., and Wakefield, W.W. 2013. A flexible sorting grid to reduce Pacific halibut
420 (*Hippoglossus stenolepis*) bycatch in the US west coast groundfish bottom trawl fishery.
421 *Fisheries Research*, 143 (2013), 102-108.
- 422 Lomeli M. J. M., and Wakefield, W.W., Herrmann, B., 2017. Testing of Two Selective Flatfish
423 Sorting-Grid Bycatch Reduction Devices in the U.S. West Coast Groundfish Bottom
424 Trawl Fishery, *Marine and Coastal Fisheries*. 9:1 597-611.
- 425 Melli, V., Herrmann, B., Karlsen, J. D., Feekings, J. P., Krag, L. A., 2020. Predicting optimal
426 combinations of by-catch reduction devices in trawl gears: A meta-analytical approach
427 *Fish and Fisheries*, 21(2) pp. 252-268
- 428 Millar, R. B. 1993. Incorporation of between-haul variation using bootstrapping and
429 nonparametric estimation of selection curves. *Fisheries Bulletin*, 91: 564–572.
- 430 Reeves, S.A., Armstrong, D.W., Fryer, R.J., and Coull, K.A., 1992. The effects of mesh size,
431 cod-end extension length and cod-end diameter on the selectivity of Scottish trawls and
432 seines *ICES J. Mar. Sci.*, 49 (1992), pp. 279-288
- 433 Robertson, J.H.B., Stewart, P.A.M., 1988. A comparison of size selection of haddock and
434 whiting by square and diamond mesh codends. *J. Cons. Int. Explor. Mer.*, 44: 148-161
- 435 Roda, M.A. P. (ed.), Gilman, E., Huntington, T., Kennelly, S.J., Suuronen, P., Chaloupka, M.
436 and Medley, P. 2019. A third assessment of global marine fisheries discards. *FAO*
437 *Fisheries and Aquaculture Technical Paper No. 633*. Rome, FAO. 78 pp.
- 438 Santos, J., Stepputtis, D., Oesterwind, D., Herrmann, B., Lichtenstein, U., Hammerl, C.,
439 Krumme, U., 2022. Reducing cod bycatch in flatfish fisheries. *Ocean and Coastal*
440 *Management — 2022*, Volume 220, pp. 106058. [10.1016/j.ocecoaman.2022.106058](https://doi.org/10.1016/j.ocecoaman.2022.106058)
- 441 Sistiaga, M., Brinkhof, J., Herrmann, B., Larsen, R. B., Grimaldo, E., Cerbule, K., Brinkhof I.,
442 Jørgensen, T., 2021. Potential for codends with shortened lastridge ropes to replace
443 mandated selection devices in demersal trawl fisheries. *Canadian Journal of Fisheries*
444 *and Aquatic Sciences*, **Just-IN**, <https://doi.org/10.1139/cjfas-2021-0178>
- 445 Sistiaga, M., Herrmann, B., Grimaldo, E., and Larsen, R. 2010. Assessment of dual selection
446 in grid based selectivity systems. *Fisheries Research*, 105: 187–199. Elsevier.

- 447 Vincent, B., Robert, M., Simon, J., Vacherot, J.P., Faillettaz, R., 2021. Exploring the mechanics
448 of fish escape attempts through mesh. *Fisheries Research* 248 (2022) 106195
449 <https://doi.org/10.1016/j.fishres.2021.106195>
- 450 Wienbeck, H., Herrmann, B., Feekings, J. P., Stepputtis, D., Moderhak, W., 2014. A
451 comparative analysis of legislated and modified Baltic Sea trawl codends for
452 simultaneously improving the size selection of cod (*Gadus morhua*) and plaice
453 (*Pleuronectes platessa*). *Fish. Res.*, 150, 28-37.
- 454 Wienbeck, H., Herrmann, B., Moderhak, W., Stepputtis D., 2011. Effect of netting direction
455 and number of meshes around on size selection in the codend for Baltic cod (*Gadus*
456 *morhua*). *Fish. Res.*, 109,80-88.
- 457 Wileman, D. A., Ferro, R. S.T., Fonteyne, R., Millar, R. B. (Eds.) 1996. Manual of Methods of
458 Measuring the Selectivity of Towed Fishing Gears. ICES Cooperative Research Report
459 No. 215. 126 pp.
- 460